ELSEVIER

Materials Science and Engineering A273–275 (1999) 430–436

MATERIALS SCIENCE & ENGINEERING A

www.elsevier.com/locate/msea

Martensite and deformation twinning in austenitic steels

V. Tsakiris [a], D.V. Edmonds [b,*]

[a] *Commercial and Logistics Department, Effem Argentina, 6608, Mercedes, Argentina*
[b] *Department of Materials, University of Leeds, Leeds, LS2 9JT, UK*

Abstract

The structural changes that occur in highly-alloyed austenitic steels during plastic deformation have been studied as a function of temperature and plastic strain. Stress-assisted and strain-induced martensites can occur, but also, deformation twinning can be identified by transmission electron microscopy. In the high-Mn austenite of Hadfield steel deformation is controlled by slip and twinning over a wide temperature range. In high-Ni and more complex alloyed austenites (such as in TRIP steels) deformation involves martensite formation, both stress-assisted and strain-induced, but near room temperature and above the influence of mechanical twinning, is also apparent.

Keywords: Austenitic steels; Plastic deformation; Martensite; Twinning

1. Introduction

Austenitic steels form an important group of industrial alloys with a broad range of properties. They contain austenite stabilising elements, e.g. Mn or Ni which open the γ-field and at sufficient concentrations preserve the fcc austenite phase at room temperature and below. The response of this stable or metastable austenite to deformation can result in enhanced properties, e.g. high work hardening or high tensile ductility, useful in a range of industrial applications. However, these properties are achieved by mechanisms involving interaction between slip and, in the highly-alloyed austenite, the potential for mechanical twinning, and also, martensite transformation induced by the deformation. Consequently, the deformation microstructures of these austenitic steels can be quite complex and the problem for early metallographers was firstly to differentiate between mechanical twinning and martensite. Mechanical twinning in fcc metals is less common but can be assisted by a high solute concentration which can simultaneously raise the shear stress for slip and reduce the stacking fault energy. Thus deformation twinning has been reported to occur, for example, in austenitic stainless steels [1–3].

Deformation twinning and deformation-induced martensitic transformation differ in that the latter is also driven by a chemical free energy change, but are microstructurally similar in that both involve diffusionless shear of a constrained plate-shaped region of parent crystal which differentiates it from the surrounding material. Additionally, they might not be expected to have such dissimilar effects on the accompanying deformation behaviour and properties of the bulk alloy. Early work on high-Mn Hadfield steel attributed a high work-hardening rate to the formation of α- or ε-martensite but the consensus of later studies [4–9] was that the microstructural striations observed were due to deformation twinning, although it has been argued more recently that the high work hardening is solely due to dynamic strain ageing [10]. On the other hand, the formation of martensite in high-Ni alloys or more complex-alloyed austenitic steels is well documented [11–17] although differentiation between strain-induced martensite and bands of twins remains a difficulty [14,15].

The present paper examines the deformation microstructures in three highly-alloyed austenites over a wide test temperature and strain range, and compares the observations and the mechanical behaviour.

* Corresponding author. Tel.: +44-113-233-2341; fax: +44-113-233-2384.
E-mail address: d.v.edmonds@leeds.ac.uk (D.V. Edmonds)

0921-5093/99/$ - see front matter
PII: S0921-5093(99)00322-6

Table 1
Chemical compositions and approximate M_s and M_d temperatures

Sample	Composition (wt.%)						M_s (°C)	M_d (°C)
	C	Si	Mn	Ni	Cr	Mo		
Hadfield steel	0.96	0.78	12.85	–	–	–	< −196	< −196
High-Ni alloy	0.6	–	–	22.8	–	–	−60	100
TRIP Steel	0.29	2.02	0.81	7.7	8.9	4.09	−196	35

2. Experimental procedures

Three steels were used, two of them based on Mn or Ni alloying with the third more complex alloyed with Ni, Cr, Mo and Si (the first composition simulates that of a Hadfield steel and the last of a transformation induced plasticity (TRIP) steel [16]). The steels were manufactured as 20 kg vacuum melts, hot forged and hot rolled to 10 mm diameter. Chemical analyses and approximate M_s and M_d temperatures are given in Table 1. The samples were sealed in evacuated silica capsules under a partial pressure of argon and heat treated and water quenched according to Table 2 which also gives the final grain sizes. Tensile specimens with a 17 mm gauge length and 3.5 mm gauge diameter were tested in an Instron 1195 machine at a nominal strain rate of 8.3×10^{-4} s^{-1}. Elevated temperature tests were conducted using a temperature-controlled resistance-heated split-furnace with the specimen temperature recorded directly by a thermocouple. Low temperature tests employed immersion in liquid nitrogen (−196°C), a mixture of ethyl alcohol and dry ice (−25– −74.5°C) and an ice–water mixture (0°C). M_s and M_d temperatures (Table 1) and the amount of martensite formed were determined by measuring the saturation magnetisation of tensile specimens before and after tensile testing [18]. Specimens for light and transmission electron microscopy were prepared according to customary practices by mechanical and electrolytic polishing and etching as detailed previously [18].

3. Results and discussion

For the high-Mn Hadfield steel the UTS, yield strength and work hardening as a function of temperature are presented in Fig. 1. The measure of work hardening used is the difference in flow stress at plastic strains of 0.04 and 0.002, and reflects the particularly high work hardenening behaviour of this steel in the range −75– +300°C. Fig. 2 shows the temperature dependence of work hardening at a range of plastic strain values and is equivalent to published results over a smaller range of conditions [10] (Adler, private communication, (1984).).

Fig. 3 shows the microstructure after 0.02 plastic strain. Similar deformation microstructures have been presented by others [4,10]. The long thin parallel-sided deformation markings, consistent with (111) type habit, variously described previously as stacking faults,

Table 2
Heat treatments and final grain sizes

Sample	Heat treatment	Grain size (μm)
Hadfield steel	1100°C for 30 min	170
High-Ni alloy	1100°C for 60 min	100
TRIP Steel	1200°C for 60 min	280

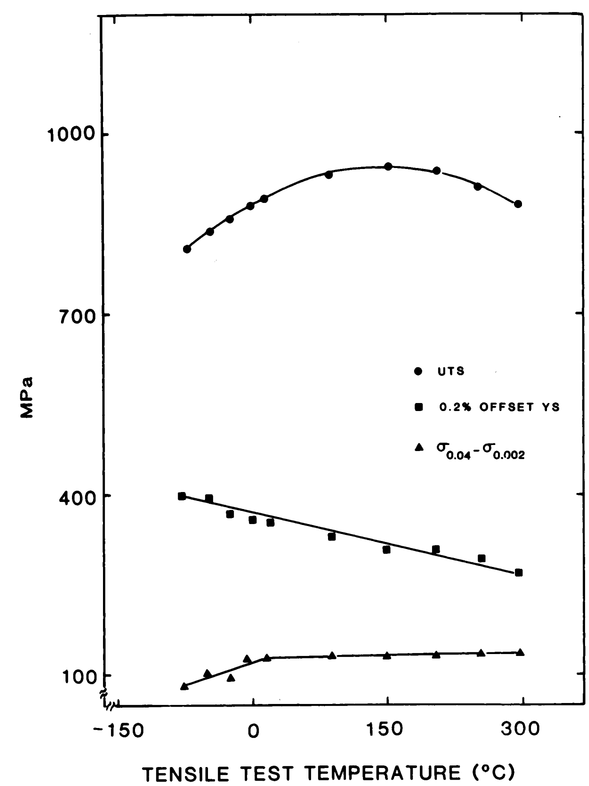

Fig. 1. UTS, yield strength and work hardening as a function of temperature for high-Mn austenite (Hadfield steel).

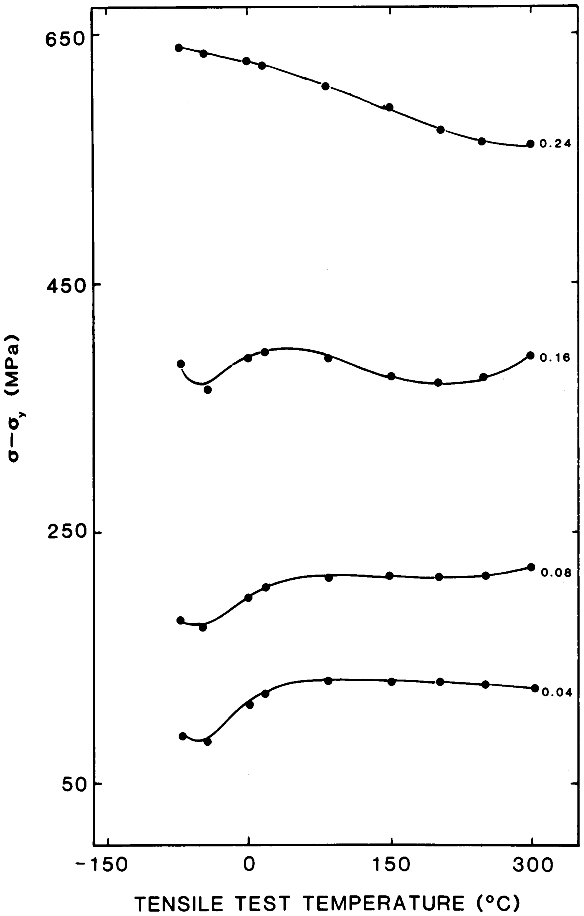

Fig. 2. Temperature dependence of work hardening at different true plastic strains for high-Mn austenite.

α- or ε-martensite, or twins, increase with strain and with decreasing temperature. Quantitative measurements indicated that these striations appear after a critical strain (which increases with temperature) and that their quantity increases parabolically and saturates

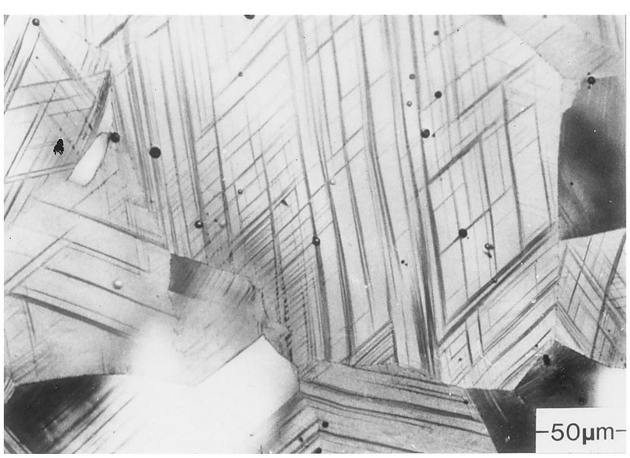

Fig. 3. Light micrograph of deformation microstructure in high-Mn austenite strained 0.02 at room temperature.

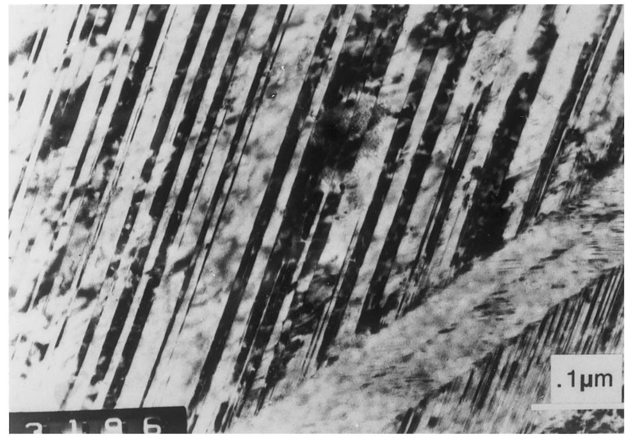

Fig. 4. Electron micrograph of high-Mn austenite strained to fracture at −25°C.

after a certain plastic strain which decreases as the temperature increases, similar to the kinetics of fcc twinning [19]. Fig. 4 is a bright-field electron micrograph of the deformed structure and shows very thin striations gathering into thicker bands along with a high dislocation density. The analysis of Fig. 5 indicates that the striations and alternate bands are twin related. The beam direction used should identify ε-martensite reflections if present [9]. Magnetic measurements also found the specimens to be fully austenitic after large plastic strains to fracture. This behaviour is consistent with measured M_s and M_d temperatures below −196°C. Consequently, the deformation markings are confirmed to be (111) deformation twinning and not martensite as occasionally reported in the past.

A maximum in work hardening around room temperature at low plastic strains is noticed in Fig. 2, which has been attributed to a unique interaction between dislocations and C–Mn couples to give dynamic strain ageing [10], consistent with the serrated plastic flow observed. However, the present results show the disappearance of this room temperature maximum at higher strains, and it is thought that this could be due to the increased influence of the profuse deformation twinning on work hardening at temperatures below room temperature. At large strains the influence of twinning on work hardening is thought to be due to the static hardening effect of twin boundaries acting as deformation barriers [8,20].

Fig. 6 illustrates the engineering stress–strain curves for the Fe–Ni–C alloy as a function of temperature. The curves are separated into two groups by different deformation mechanisms and this is also reflected in the work hardening behaviour presented in Fig. 7. At small plastic strains <0.08 the low temperature hardening is high due to stress-assisted martensite formation which at −50°C, near the M_s, has caused large serrations before yield on the stress-strain curve. At lower test

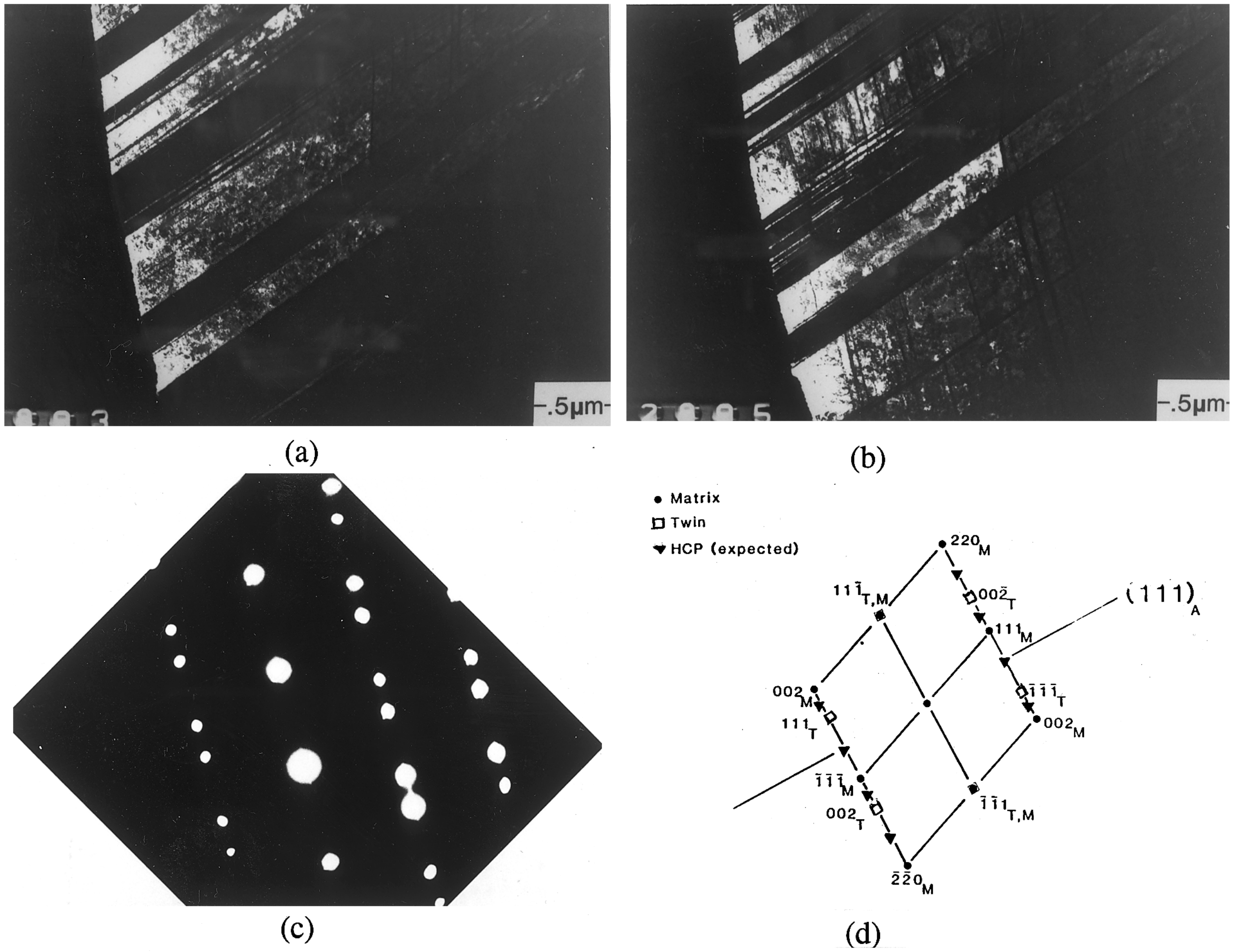

Fig. 5. Dark-field electron micrographs of banded structure in high-Mn austenite using: (a) 111_M, and (b) 111_T reflections; (c) diffraction pattern and (d) analysis (triangular symbols indicate the position of hcp ε-martensite reflections if present).

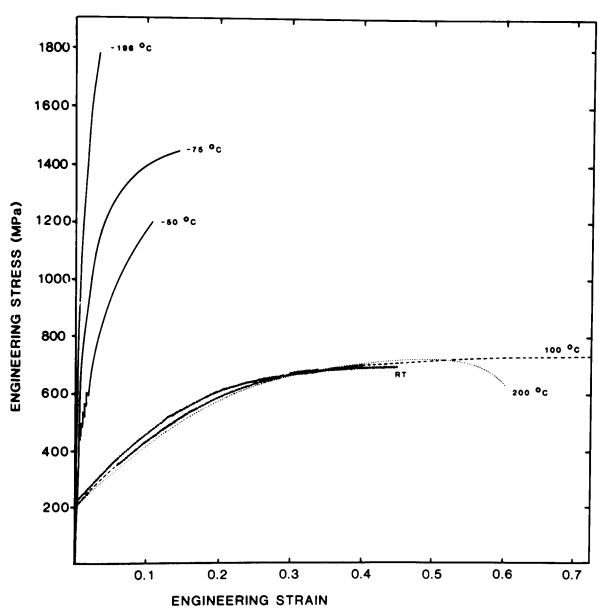

Fig. 6. Engineering stress–strain curves for high-Ni austenite tested at various temperatures.

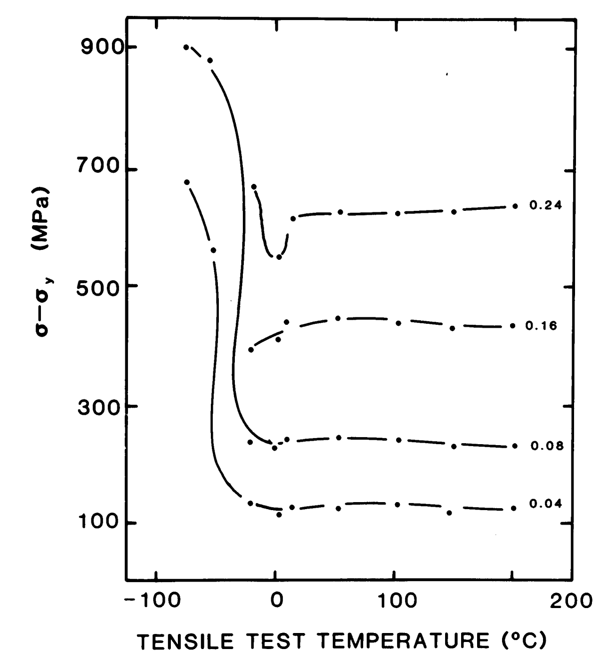

Fig. 7. Temperature dependence of work hardening at different true plastic strains for high-Ni austenite.

temperatures, $< M_s$, the reduction in available austenite is thought to minimise serrations [21]. This stress-assisted broad lenticular plate-like bcc martensite is illustrated by Fig. 8. Static hardening of the austenite by the martensite plates coupled with the hardness of the bcc martensite itself dominates the mechanical behaviour and tensile ductility is limited. At room temperature (near the upper temperature limit for stress-assisted martensite, M_s^σ [22]), and above, (with M_d around 100°C) the deformation behaviour is thought to be dominated by the austenite. The fine serrations in the stress–strain curve after yielding apparent at 0 and 100°C are consistent with (111) deformation twinning (Fig. 9) but evidence for significant strain-induced martensite below 100°C was also found, although saturation magnetisation measurements indicated $< 20\%$ (even lower amounts have been measured by others [12,13]) allowing austenite slip and twinning mechanisms to dominate. Identification of the strain bands as deformation twinning confirms previous work [14,23] but differs from others [12,13,15] who ascribed it to strain-induced martensite, however, these studies were either carried out close to M_s^σ or misinterpreted the diffraction evidence [23]. Fig. 9 is from a specimen deformed at 100°C where no alternative evidence for martensite formation was observed. It is also noticed that the total elongation exhibits a maximum at 100°C and this may be attributed to enhancement of uniform elongation by the increased work hardening due to the profuse deformation twinning.

A comparison of the room temperature deformation in the high-Mn and high-Ni alloys shows them both to exhibit serrated flow and to have equivalent work hardening up to a plastic strain of 0.06. This is consistent with deformation twinning in the austenites, confirmed to occur, although there is the possibility of strong dynamic strain ageing in one alloy [10] and strain-induced martensite in the other.

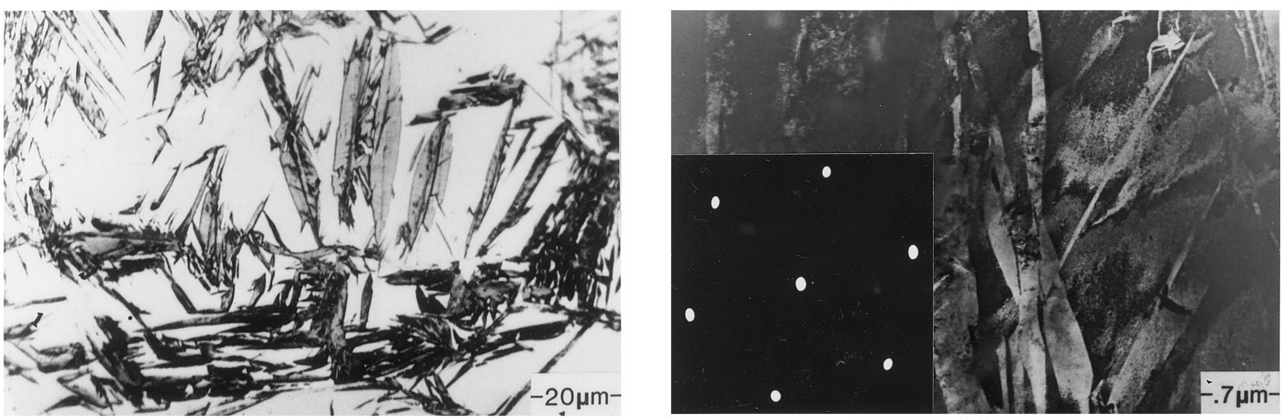

(a) (b)

Fig. 8. Deformation microstructure in high-Ni austenite strained to fracture at: (a) −40°C, light micrograph, and (b) −20°C, electron micrograph.

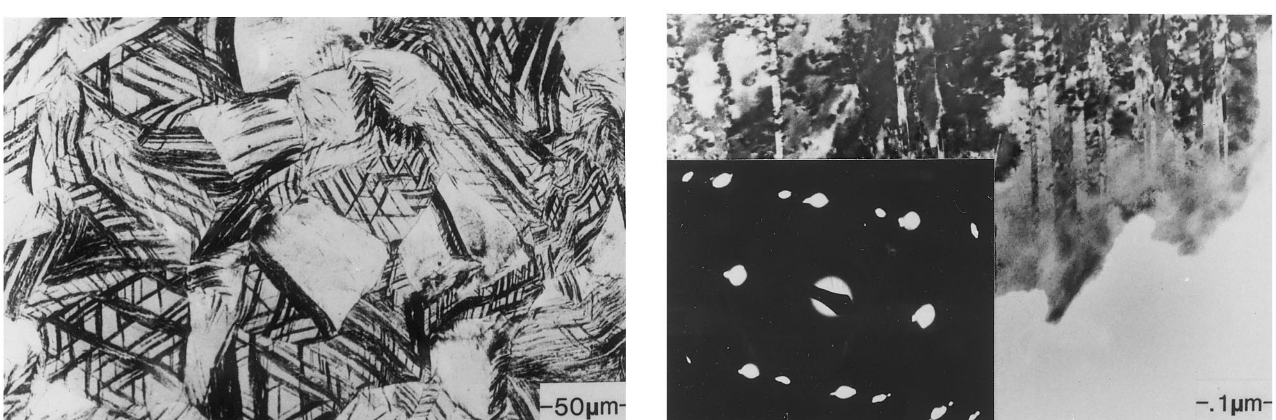

(a) (b)

Fig. 9. Banded structure in high-Ni austenite strained to fracture at 100°C: (a) light micrograph, and (b) electron micrograph.

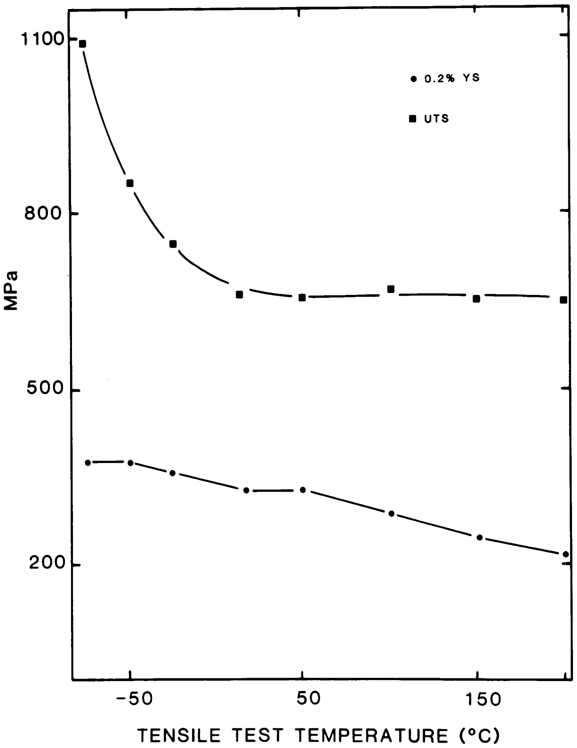

Fig. 10. UTS and yield strength as a function of temperature for complex-alloyed austenite (TRIP steel).

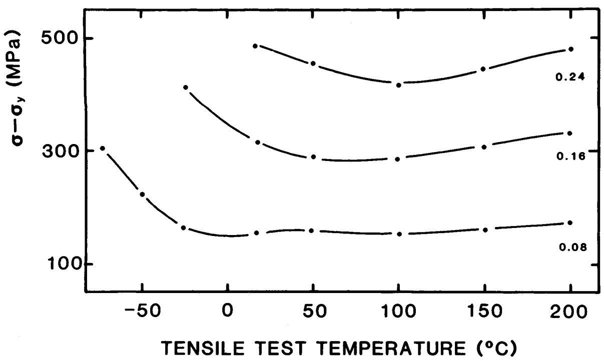

Fig. 11. Temperature dependence of work hardening at different true plastic strains for complex-alloyed austenite.

The simulated TRIP steel has a low M_s (-196°C) but relatively high M_d (35°C). The UTS shows a strong temperature dependence beneath room temperature (Fig. 10) characteristic of metastable austenite [24] which is a reflection of the high work hardening (Fig. 11). Magnetic measurements indicated strain-induced martensite and evidence for this was also found metallographically as shown in Fig. 12, which is similar to the appearance found by others [17]. Electron diffraction studies confirmed bcc martensite. The mechanical behaviour is also not dissimilar to that previously recorded and explained through the influence of strain-induced martensite alone [17,25]. However, in the present study fine bands similar in morphology to those found in the other alloys were also detected as shown in Fig. 13 and identified as (111) deformation twins.

4. Summary

Mechanical behaviour in a range of highly-alloyed austenites is shown to be influenced by deformation twinning as well as deformation-induced martensite transformation. Deformation twinning is operative in a high-Mn Hadfield steel over a broad temperature and strain range, and can combine with any unique strain ageing effects to result in the characteristic high work hardening. In a high-Ni austenite with M_s and M_d temperatures spanned by the test temperature range an influence of both stress-assisted and strain-induced martensite, along with deformation twinning, is found. In the austenite of a complex-alloyed TRIP steel with M_d just above room temperature the mechanical behaviour at room temperature and below is strongly influenced by strain-induced martensite although deformation twinning was still evident.

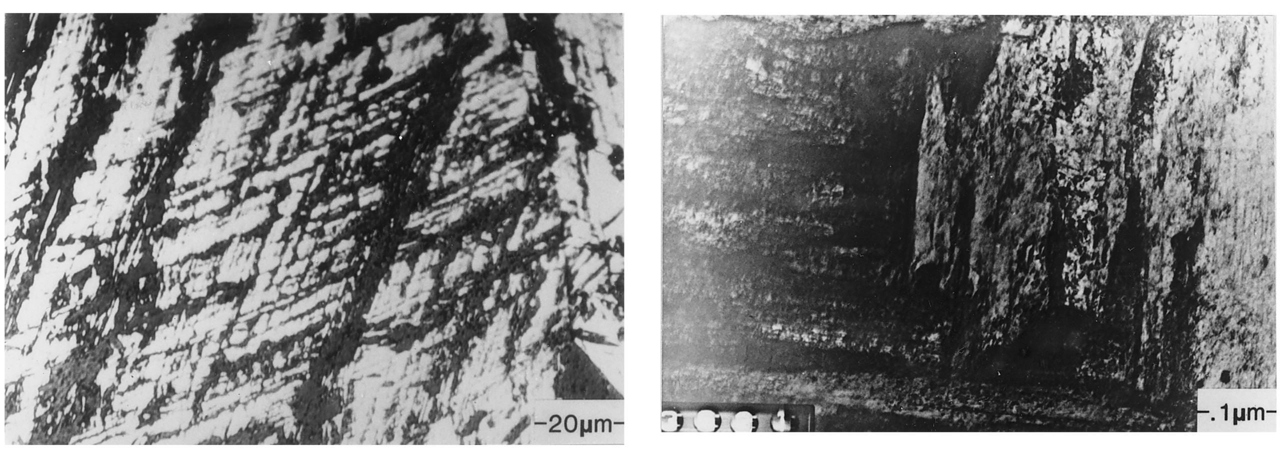

(a) (b)

Fig. 12. Deformation microstructure in complex-alloyed austenite strained to fracture at -25°C: (a) light micrograph and (b) electron micrograph.

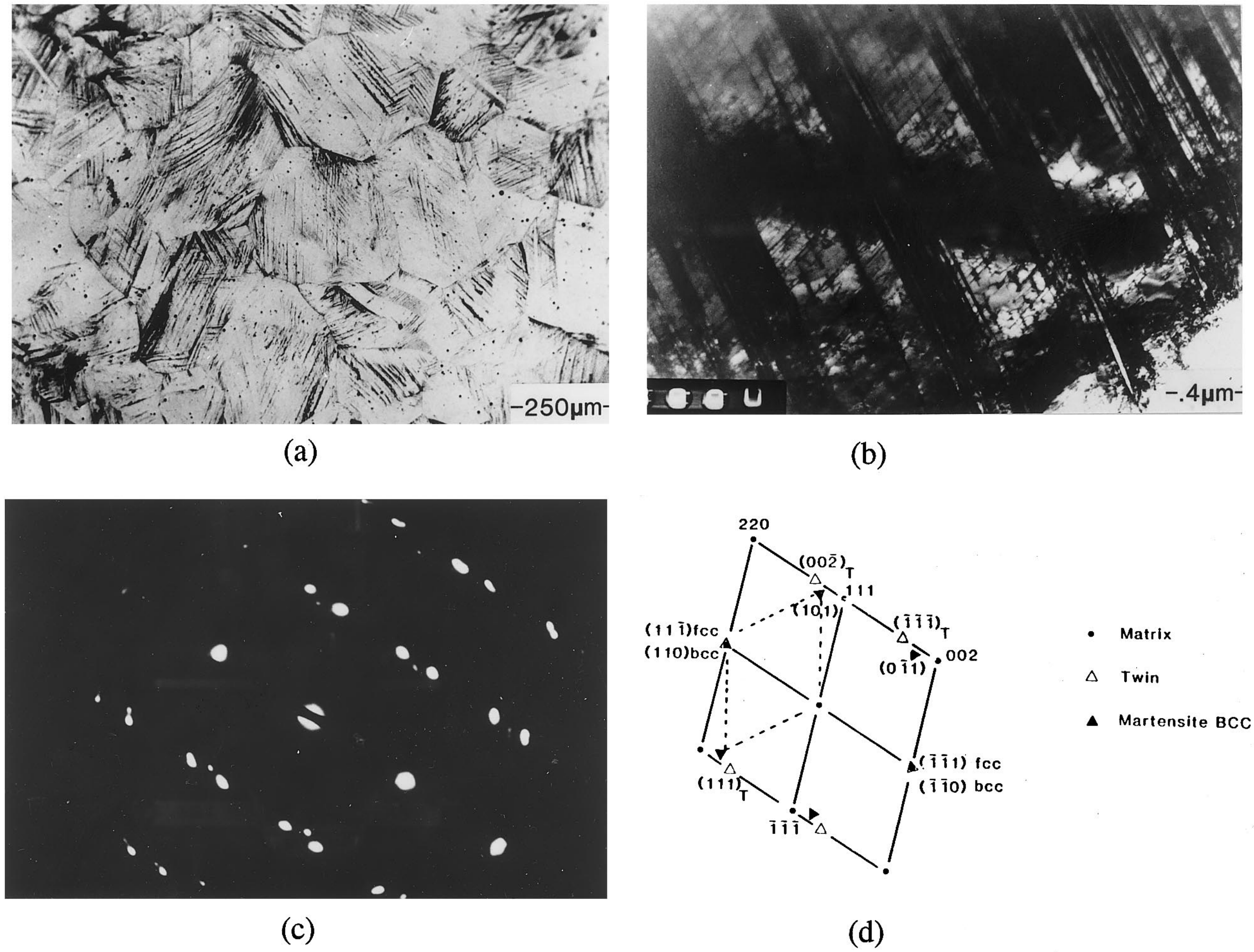

Fig. 13. Banded structure in complex-alloyed austenite strained to fracture at room temperature: (a) light micrograph, (b) electron micrograph, (c) diffraction pattern and (d) analysis.

References

[1] L.E. Murr, K.P. Staudhammer, S.S. Hecker, Metall. Trans. 13A (1982) 627.
[2] K.P. Staudhammer, L.E. Murr, S.S. Hecker, Acta Metall. 31 (1983) 267.
[3] P. Maulik, J. Burke, A.W. Thompson, Scr. Metall. 17 (1983) 233.
[4] H.M. Otte, Acta Metall. 5 (1957) 614.
[5] C.H. White, R.W.K. Honeycombe, J. Iron Steel Inst. 200 (1962) 457.
[6] W.N. Roberts, Trans. AIME 230 (1964) 372.
[7] Z. Nishiyama, M. Oka, H. Nakagawa, Trans. JIM 6 (1965) 88.
[8] K.S. Raghavan, A.S. Sastri, M.J. Markinkowski, Trans. AIME 245 (1969) 1569.
[9] H.J. Kestenbach, Metallography 10 (1977) 189.
[10] Y.N. Dastur, W.C. Leslie, Metall. Trans. 12A (1981) 749.
[11] T. Maki, S. Shimooka, M. Umemoto, I. Tamura, Trans. JIM 13 (1972) 400.
[12] P.C. Maxwell, A. Goldberg, J.C. Shyne, Metall. Trans. 5 (1974) 1305.
[13] P.C. Maxwell, A. Goldberg, J.C. Shyne, Metall. Trans. 5 (1974) 1319.
[14] H. Onodera, I. Tamura, Scr. Metall. 11 (1977) 1057.
[15] T.N. Durlu, Scr. Metall. 15 (1981) 689.
[16] V.F. Zackay, E.R. Parker, D. Fahr, R. Busch, Trans. ASM. 60 (1967) 252.
[17] G.B. Olson, M. Azrin, Metall. Trans. 9A (1978) 713.
[18] V. Tsakiris, PhD Thesis, University of Oxford, 1986.
[19] L. Remy, Acta Metall. 26 (1978) 443.
[20] L.E. Murr, F.I. Grace, Trans. AIME 245 (1969) 2225.
[21] I. Tamura, T. Maki, H. Hato, Trans. Jap. ISI 10 (1970) 163.
[22] G.F. Bolling, R.H. Richman, Scr. Metall. 4 (1970) 539.
[23] A.K. Sachdev, M.M. Shea, Metall. Trans. 16A (1985) 445.
[24] J.P. Bressanelli, A. Moskowitz, Trans. ASM. 59 (1966) 223.
[25] G.R. Chanani, V.F. Zackay, E.R. Parker, Metall. Trans. 2 (1972) 133.